PROCEEDINGS OF SCIENCE

Latest Advancements on Cosmic Ray Carbon and Oxygen with the DAMPE space mission

D. Kyratzis,[a,b,*] **C. Yue,**[c] **Y. Wei,**[d,e] **A. Serpolla**[f] **and I. De Mitri**[a,b] **on behalf of the DAMPE collaboration**

[a] *Gran Sasso Science Institute (GSSI), Via Iacobucci 2, 67100, L'Aquila, Italy*
[b] *INFN, Laboratori Nazionali del Gran Sasso (LNGS), 67100 Assergi, L'Aquila, Italy*
[c] *Key Laboratory of Dark Matter and Space Astronomy, Purple Mountain Observatory, Chinese Academy of Sciences, Nanjing 210023, China*
[d] *State Key Laboratory of Particle Detection and Electronics, University of Science and Technology of China, Hefei 230026, China*
[e] *Department of Modern Physics, University of Science and Technology of China, Hefei 230026, China*
[f] *Department of Nuclear and Particle Physics, University of Geneva, CH-1211 Geneva, Switzerland*

E-mail: dimitrios.kyratzis@gssi.it, dimitrios.kyratzis@cern.ch

The Dark Matter Particle Explorer (DAMPE), is a space–borne detector designed for precise Galactic Cosmic Ray (GCR) studies in a wide energy range (up to a few hundreds of TeV), along with detailed measurements of high–energy gamma–rays and indirect searches of Dark Matter (DM). The satellite was successfully launched into a sun–synchronous orbit at 500 km, on December 17th 2015 and has been successfully taking data ever since.

DAMPE can provide valuable insights on the energy spectra of medium mass nuclei (CNO group) with exceptional resolution. In this work, the latest advancements regarding the spectral measurement of carbon and oxygen nuclei, will be presented, along with additional insights on the C/O flux ratio and the collective CNO flux, with 9 years of DAMPE flight data. Said results are crucial in deciphering distinct features across all spectra, complimented by a significant extension into the multi-TeV/n region, with great accuracy.

39th International Cosmic Ray Conference (ICRC2025)
15–24 July 2025
Geneva, Switzerland

ICRC 2025
The Astroparticle Physics Conference
Geneva July 15-24, 2025

*Speaker

PoS(ICRC2025)061

1. Introduction

Cosmic ray (CR) studies comprise a significant part of rigorous research activities, with fundamental open questions concerning their origin, acceleration and propagation mechanisms in the Galaxy [1]. Constituting the majority of CRs, protons and helium nuclei were thoroughly investigated by DAMPE. The published spectrum of protons [2] (energy range: 40 GeV - 100 TeV), lead to the detection of a spectral hardening around 500 GeV (consistent with previous observations) along with a novel softening featured approximately at 14 TeV. The aforementioned characteristics were described by a smoothly-broken power-law (SBPL) model above the observed hardening, hence ruling-out the previously favored paradigm of a single power-law governing CR spectra up to PeV energies. Additionally, DAMPE presented a detailed spectral measurement of helium nuclei [3] (energy range: 70 GeV - 80 TeV), revealing an analogous picture as in the proton case; a hardening feature around 1 TeV in accordance with previous results, followed by a spectral softening around 34 TeV. Exploring the nature and behavior of the most abundant primaries after protons and helium nuclei is crucial, in order to investigate possible similarities to the aforementioned spectra, while examining the validity of CR models foreseeing a rigidity-wise acceleration of particles at the sources. Consequently, this work will illustrate the latest advancements towards the measurement of carbon and oxygen nuclei (along with their respective C/O flux ratio) with DAMPE, utilizing nine years of flight data.

2. The Dark Matter Particle Explorer

DAMPE [4] is a space-borne detector designed for direct detection of Galactic CRs, while providing insights on gamma rays and possible indirect signatures of Dark Matter (DM). On December 17th, 2015, the payload was successfully injected in a sun-synchronous, Low-Earth Orbit (LEO), at an altitude of 500 km, with an inclination angle of 97.4 degrees. Following the complete range of consistent ground and on-orbit calibrations [5], the detector is operating in a stable manner throughout its lifetime, thus allowing for high quality data collection. The experiment aims to address open questions and assist in current efforts concerning: (1) a deeper understanding of the acceleration mechanism of particles in stellar environments, while realizing the nature of propagation of CRs in the Interstellar Medium, (2) detecting gamma ray signatures of galactic and extragalactic origin and (3) probing the essence of Dark Matter by its annihilation/decay in observable particles. The DAMPE instrument is able to detect electrons, positrons and gamma rays in the energy range of approximately 5 GeV to 10 TeV and protons with heavier nuclei spanning from few tens of GeV to few hundreds of TeV. The payload consists of four sub-detectors (starting from the top): a Plastic Scintillator Detector (PSD) [6], a Silicon-Tungsten tracKer-converter (STK) [7], a Bismuth Germanium Oxide (BGO) calorimeter (32 X_0 and 1.6 λ_I), along with a NeUtron Detector (NUD). The PSD is configured to precisely measure the charge as well as providing an effective veto in the case of gamma rays. The STK accurately reconstructs charged particle tracks and converts incoming gamma-rays into electron-positron pairs while providing an additional charge measurement. Charged CRs should deposit their energy inside the BGO calorimeter, by means of electromagnetic or hadronic cascades, while providing valuable insights on particle identification.

Finally, an additional level of electron-hadron discrimination from showers initiated in the BGO is achieved with the NUD.

3. Analysis selections

The analysis of carbon and oxygen nuclei presented in this work is based on nine years of DAMPE flight data collected between January 1, 2016 and December 31, 2024, with the instrument livetime amounting to 76% (or $\sim 2 \times 10^8$ s) of its total orbit. Following the retrieval of analysis-ready datasets, the entirety of poorly reconstructed and/or geometrically inconsistent events are removed, as well as events passing through the South Atlantic Anomaly (SAA) region, in order to reduce overall data size. Candidate tracks are required to activate the High Energy Trigger (HET)[1] and lie within the PSD, STK and BGO fiducial volumes. A dedicated Machine Learning (ML) algorithm [8] has been developed for DAMPE in order to handle the track reconstruction of impinging particles, demonstrating optimal performance along with a significant increase in acceptance.

Events depositing their maximum energy at the edge of the calorimeter concerning layers 1-2-3[2] are rejected, while the maximum energy deposited in any single BGO layer must remain below 35% of the total, to suppress side-entering events and maintain a well-contained shower core. In order to reject upward-oriented showers produced by particle interactions with the BGO bars, the combined energy deposited in the first and second layers is required to be smaller than that in the third and fourth layers, i.e. $E_{L0} + E_{L1} < E_{L2} + E_{L3}$. Additionally, candidate events depositing less than 70 GeV (E_{BGO}) are excluded to avoid contamination from the geomagnetic rigidity cutoff and solar energetic particles. Moreover, a fixed threshold of 500 ADC (Analog-to-Digital-Converter) for particles impinging on either X or Y planes of the first STK layer, is imposed, in order to mitigate the contribution of lighter than beryllium nuclei and minimize the overall background contamination.

3.1 Progressing PSD charge selection

CR nuclei impinging on the PSD, give rise to a multitude of interactions according to their incident energy and mass. When moving from lighter to heavier nuclei, the probability of nuclear fragmentation becomes more prominent, hence introducing a sizable charge distortion in the selected events. An intricate method of determining the PSD charge is developed in this analysis, following an event-by-event approach which aims at registering layer-consistent charge measurements, while avoiding potential loss of fragmented events in the process. The so-called progressing PSD charge method can be given by:

$$Q^{PSD} = \frac{\sum_i Q_i^{PSD}}{\sum_i N_{Layers}} \tag{1}$$

[1] The High Energy Trigger, requests an energy deposition greater than 10 MIPs (one MIP corresponding to 23 MeV) in each one of the first three BGO layers and 2 MIPs for the fourth layer.

[2] BGO layer numbering starts from zero.

where Q^{PSD} is the final PSD charge and Q_i^{PSD} corresponds to the charge value found in a given layer, with $\sum_i N_{Layers}$ signaling the number of consecutive PSD layers giving a non-zero charge. At the same time, a consistency check between signals in adjacent layers: $\left|Q_i^{PSD} - Q_{i+1}^{PSD}\right| < 2$ which requires events registered in neighboring layers to be within two absolute charge units, thus eliminating possible inconsistencies arising mainly from fragmentation interactions or spurious events in the detector.

3.2 DAMPE simulated data

The simulated events used in this analysis are based on GEANT4 (version 10.05p01) [9] coupled to the DAMPE software [10, 11], being the dedicated collaboration framework. All events concerning carbon and oxygen nuclei were simulated in the energy range of 20 GeV to 1 PeV. The large majority of events were produced with the FTFP_BERT physics list (from 20 GeV to 100 TeV of primary particle energy), while for energies greater than 100 TeV, the EPOS_LHC model is employed. It should be noted that carbon and oxygen samples of similar event count and energy intervals were also produced and analyzed with FLUKA [12].

3.3 Background estimation

An integrated model is constructed in order to accurately describe individual background contributions for the nuclei of interest. Such a method provides an optimal determination of the charge selection bounds, taking into account the lowest possible contamination. The procedure concerning individual templates according to a given energy bin requires a careful inclusion of all MC simulated and flight PSD charge histograms. Following the definition of the probability density function, a strict scaling (no bin fluctuations or data compensations are allowed) based on each individual MC template can be obtained, using RooFit [13]. In each BGO energy bin a constant PSD charge selection is imposed, in order to accurately gauge the background contamination. The various templates according to the energy deposited in the calorimeter are shown in Fig. 1, while the final background estimation for carbon and oxygen nuclei is shown in Fig. 2. Both selections amount to very low contamination percentages, ranging from less than 0.1% to a maximum of 3 - 4% for the highest deposited energies.

3.4 Preliminary uncertainty evaluation

In order to carefully assess the statistical uncertainties in carbon and oxygen data, a Toy MC method is employed by generating simulated samples from Poisson distributions with mean values equal to the dataset of flight data, in order to evaluate possible fluctuations with respect to each BGO energy bin, during spectral unfolding. The unfolding method is employed despite the extended calorimetric depth of DAMPE and its excellent resolution, since only a fraction of the energy corresponding to the primary particle can be contained within the BGO layers ($\sim 40\%$ at 10 TeV). Such aspects necessitate the implementation of unfolding methods in order to obtain a precise spectrum regarding the impinging primary element of interest. Results presented in this work are based on an iterative Bayesian method [14].

Systematic uncertainties from the unfolding procedure, charge definition, background contamination, HET activation as well as the various selection cuts in PSD, STK and BGO have been

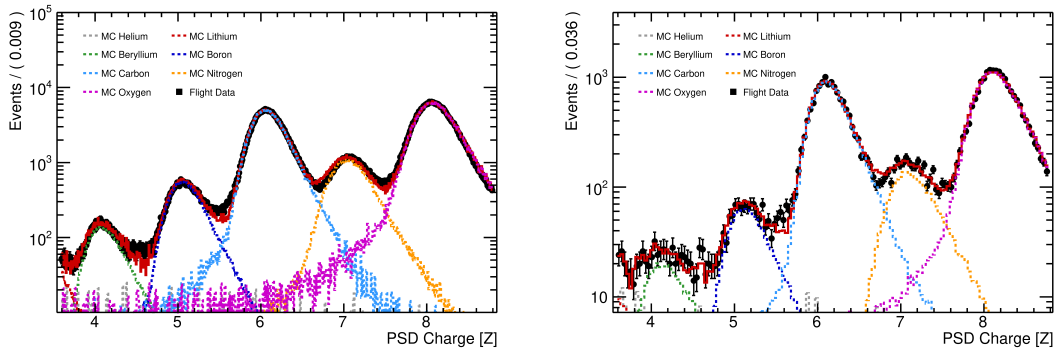

(a) (b)

Figure 1: PSD spectra including contributions from helium to oxygen nuclei (focusing on the vicinity of the CNO group) concerning flight and simulated data in various energy bins (BGO energy), specifically illustrated in the range of (a) 178 - 316 GeV and (b) 1.78 - 3.16 TeV. The various colored lines correspond to MC samples, black points refer to flight data, while the red continuous line represents the optimal template fit.

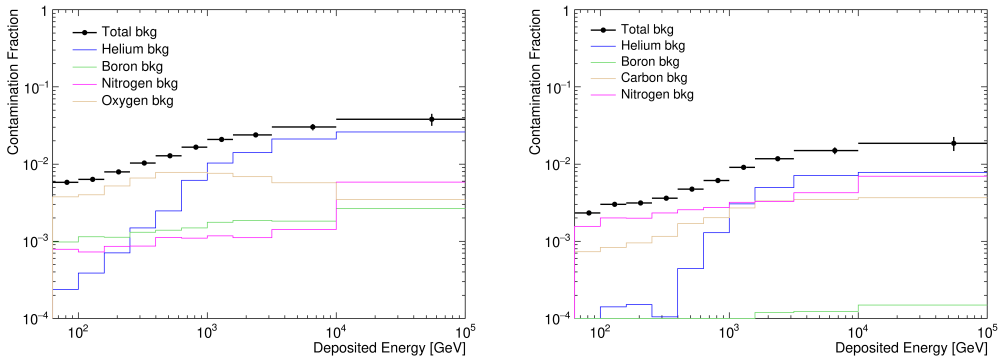

(a) (b)

Figure 2: Preliminary background contamination fractions for (a) carbon and (b) oxygen nuclei according to the final charge selection.

measured in detail. Regarding the systematics stemming from the hadronic model of choice, a synergy between FLUKA and beam test data acquired during the various beam test campaigns at CERN has been adopted, in order to accurately evaluate the aforementioned contribution in the full energy range. The collective uncertainty estimation will be included in the preliminary fluxes, as shown in the following section.

4. Preliminary Carbon and Oxygen fluxes

The final flux measurement for carbon and oxygen nuclei is given by the following formula:

$$\Delta\Phi\left(E_i, E_i + \Delta E_i\right) = \frac{\Delta \mathrm{N_i}}{\Delta \mathrm{E_i}\ \mathrm{A_{eff},}_i \Delta \mathrm{T}} \tag{2}$$

where $[E_i, E_i + \Delta E_i]$ corresponds to the i-th primary energy bin with a step of ΔE_i, while ΔN_i is the number of carbon or oxygen events surviving all selection cuts introduced in previous sections. $\mathrm{A_{eff},}_i$ is the effective acceptance which includes the geometric acceptance along with the efficiency of all applied cuts and finally, ΔT is the total instrument livetime, corresponding to 9 years of DAMPE data, as seen in Fig. 3(a) for Carbon, Fig. 3(b) for Oxygen and Fig. 3(c) for the C/O flux ratio. The latest DAMPE results are presented alongside published works of CREAM [15], PAMELA [16], NUCLEON [17], CALET [18] and AMS-02 [19] experiments.

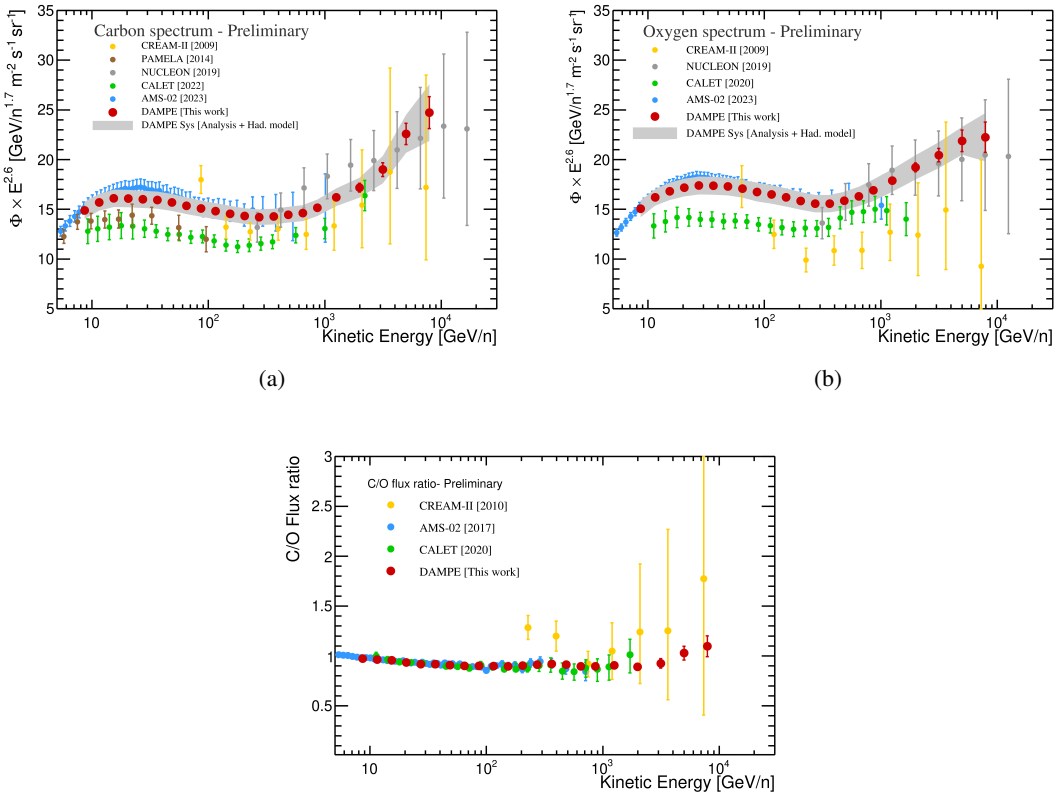

Figure 3: Preliminary DAMPE spectra of CR (a) carbon, (b) oxygen and their respective flux ratio (c) C/O, with 9 years of flight data. Both fluxes are multiplied to $\mathrm{E}^{2.6}$, red error bars represent statistical uncertainties while the gray-shaded band refers to the total systematic uncertainty estimated from analysis and hadronic model selections, added in quadrature. The published works of CREAM [15], PAMELA [16], NUCLEON [17], CALET [18] and AMS-02 [19] experiments are shown for a detailed comparison.

5. Conclusion

In this work, the latest advancements regarding CR carbon and oxygen, with 9 years of DAMPE flight data have been presented, in the energy range of 7.5 GeV/n to 7.9 TeV/n. A hardening feature is evident at energies of approximately 300 GeV/n, the shape of which is consistent with AMS-02 and CALET observations. Such a feature invalidates the conventional picture involving a universal injection spectrum at the sources and a single, featureless power-law spectrum extending up to PeV energies, as predicted by prevalent CR models. These results are coherent with published DAMPE measurements of protons and helium nuclei in a similar energy range. Both carbon and oxygen fluxes are found to be in good agreement with AMS-02 results (up to the TeV/n region), within the estimated uncertainties, with DAMPE data extending well into the multi-TeV/n region with great accuracy. An additional result stemming from the analysis is associated to the carbon-over-oxygen ratio, being in agreement with the majority of published results especially in lower energies, while exhibiting an increasing tendency towards the multi-TeV/n region.

Acknowledgments

The DAMPE mission was funded by the strategic priority science and technology projects in space science of Chinese Academy of Sciences. In China the data analysis is supported by the National Key Research and Development Program of China (No. 2022YFF0503302), the National Natural Science Foundation of China No. 12220101003, No. 12275266, No. 12003076, No. 12022503, and No. 12103094), the Strategic Priority Program on Space Science of Chinese Academy of Sciences (No. E02212A02S), the Youth Innovation Promotion Association of CAS and the New Cornerstone Science Foundation through the XPLORER PRIZE. In Europe the activities and data analysis are supported by the Swiss National Science Foundation (SNSF), Switzerland, the National Institute for Nuclear Physics (INFN), Italy, and the European Research Council (ERC) under the European Union's Horizon 2020 research and innovation program (No. 851103).

References

[1] R. Aloisio, P. Blasi, I. De Mitri, and S. Petrera, *Selected Topics in Cosmic Ray Physics*, pp. 1–95. Cham: Springer International Publishing, 2018.

[2] Q. An, R. Asfandiyarov, P. Azzarello, P. Bernardini, X. Bi, M. Cai, J. Chang, D. Chen, H. Chen, J. Chen, *et al.*, "Measurement of the cosmic ray proton spectrum from 40 gev to 100 tev with the dampe satellite," *Science advances*, vol. 5, no. 9, p. eaax3793, 2019.

[3] F. Alemanno *et al.*, "Measurement of the Cosmic Ray Helium Energy Spectrum from 70 GeV to 80 TeV with the DAMPE Space Mission," *Phys. Rev. Lett.*, vol. 126, p. 201102, 2021.

[4] J. Chang *et al.*, "The DArk Matter Particle Explorer mission," *Astropart. Phys.*, vol. 95, pp. 6–24, 2017.

[5] G. Ambrosi *et al.*, "Direct detection of a break in the teraelectronvolt cosmic-ray spectrum of electrons and positrons," *Nature*, vol. 552, pp. 63–66, 2017.

[6] Y. Yu, Z. Sun, H. Su, Y. Yang, J. Liu, J. Kong, G. Xiao, X. Ma, Y. Zhou, H. Zhao, *et al.*, "The plastic scintillator detector for dampe," *Astroparticle Physics*, vol. 94, pp. 1–10, 2017.

[7] P. Azzarello, G. Ambrosi, R. Asfandiyarov, P. Bernardini, B. Bertucci, A. Bolognini, F. Cadoux, M. Caprai, I. De Mitri, M. Domenjoz, *et al.*, "The dampe silicon–tungsten tracker," *Nuclear Instruments and Methods in Physics Research Section A: Accelerators, Spectrometers, Detectors and Associated Equipment*, vol. 831, pp. 378–384, 2016.

[8] A. Tykhonov *et al.*, "A deep learning method for the trajectory reconstruction of cosmic rays with the dampe mission," *Astroparticle Physics*, vol. 146, p. 102795, 2023.

[9] S. Agostinelli, J. Allison, K. a. Amako, J. Apostolakis, H. Araujo, P. Arce, M. Asai, D. Axen, S. Banerjee, G. . Barrand, *et al.*, "Geant4—a simulation toolkit," *Nuclear instruments and methods in physics research section A: Accelerators, Spectrometers, Detectors and Associated Equipment*, vol. 506, no. 3, pp. 250–303, 2003.

[10] C. Wang *et al.*, "Offline software for the dampe experiment," *Chinese Physics C*, vol. 41, no. 10, p. 106201, 2017.

[11] A. Tykhonov, "Offline and cad-geant4 software of the dampe mission," in *XXVII International Symposium on Lepton Photon Interactions at High Energies*, vol. 245, p. 104, SISSA Medialab, 2016.

[12] A. Ferrari, P. Sala, A. Fasso, and J. Ranft, "Fluka: a multi-particle transport code," *CERN Yellow report*, vol. 2005-10, 2005.

[13] S. Hageböck, "What the new roofit can do for your analysis," in *Proceedings of Science (ICHEP2020)*, vol. 390, p. 910, 2021.

[14] G. D'Agostini, "A multidimensional unfolding method based on bayes' theorem," *Nuclear Instruments and Methods in Physics Research Section A: Accelerators, Spectrometers, Detectors and Associated Equipment*, vol. 362, no. 2-3, pp. 487–498, 1995.

[15] H. S. Ahn *et al.*, "Energy spectra of cosmic-ray nuclei at high energies," *The Astrophysical Journal*, vol. 707, no. 1, p. 593, 2009.

[16] O. Adriani *et al.*, "Measurement of boron and carbon fluxes in cosmic rays with the pamela experiment," *The Astrophysical Journal*, vol. 791, no. 2, p. 93, 2014.

[17] D. Karmanov, I. Kovalev, I. Kudryashov, A. Kurganov, A. Panov, D. Podorozhny, A. Turundaevskiy, and O. Vasiliev, "Spectra of cosmic ray carbon and oxygen nuclei according to the nucleon experiment," *Physics Letters B*, vol. 811, p. 135851, 2020.

[18] Y. Akaike, O. Adriani, *et al.*, "The calorimetric electron telescope (calet) on the international space station: Results from the first eight years on orbit," *Advances in Space Research*, vol. 74, no. 9, pp. 4353–4367, 2024.

[19] M. Aguilar *et al.*, "Properties of cosmic-ray sulfur and determination of the composition of primary cosmic-ray carbon, neon, magnesium, and sulfur: Ten-year results from the alpha magnetic spectrometer," *Phys. Rev. Lett.*, vol. 130, p. 211002, 2023.

DAMPE Collaboration

Francesca Alemanno[1,2], Qi An[3,4], Philipp Azzarello[5], Felicia-Carla-Tiziana Barbato[6,7], Paolo Bernardini[1,2], Xiao-Jun Bi[8,9], Hugo Valentin Boutin[5], Irene Cagnoli[6,7], Ming-Sheng Cai[10,11], Elisabetta Casilli[1,2*], Jin Chang[10,11], Deng-Yi Chen[10], Jun-Ling Chen[12], Zhan-Fang Chen[12], Zi-Xuan Chen[12,8], Paul Coppin[5], Ming-Yang Cui[10], Tian-Shu Cui[13], Ivan De Mitri[6,7], Francesco de Palma[1,2], Adriano Di Giovanni[6,7], Tie-Kuang Dong[10], Zhen-Xing Dong[13], Giacinto Donvito[14], Jing-Lai Duan[12], Kai-Kai Duan[10], Rui-Rui Fan[9], Yi-Zhong Fan[10,11], Fang Fang[12], Kun Fang[9], Chang-Qing Feng[3,4], Lei Feng[10], Sara Fogliacco[6,7], Jennifer-Maria Frieden[5†], Piergiorgio Fusco[14,15], Min Gao[9], Fabio Gargano[14], Essna Ghose[1,2], Ke Gong[9], Yi-Zhong Gong[10], Dong-Ya Guo[9], Jian-Hua Guo[10,11], Shuang-Xue Han[13], Yi-Ming Hu[10], Guang-Shun Huang[3,4], Xiao-Yuan Huang[10,11], Yong-Yi Huang[10], Maria Ionica[16], Lu-Yao Jiang[10], Wei Jiang[10], Yao-Zu Jiang[16‡], Jie Kong[12], Andrii Kotenko[5], Dimitrios Kyratzis[6,7], Shi-Jun Lei[10], Bo Li[10,11], Manbing Li[5], Wei-Liang Li[13], Wen-Hao Li[10], Xiang Li[10,11], Xian-Qiang Li[13], Yao-Ming Liang[13], Cheng-Ming Liu[16], Hao Liu[10], Jie Liu[12], Shu-Bin Liu[3,4], Yang Liu[10], Francesco Loparco[14,15], Miao Ma[13], Peng-Xiong Ma[10], Tao Ma[10], Xiao-Yong Ma[13], Giovanni Marsella[1,2§], Mario-Nicola Mazziotta[14], Dan Mo[12], Yu Nie[3,4], Xiao-Yang Niu[12], Andrea Parenti[6,7¶], Wen-Xi Peng[9], Xiao-Yan Peng[10], Chiara Perrina[5‖], Enzo Putti-Garcia[5], Rui Qiao[9], Jia-Ning Rao[13], Yi Rong[3,4], Andrea Serpolla[5], Ritabrata Sarkar[6,7], Pier-paolo Savina[6,7], Zhi Shangguan[13], Wei-Hua Shen[13], Zhao-Qiang Shen[10], Zhong-Tao Shen[3,4], Leandro Silveri[6,7**], Jing-Xing Song[13], Hong Su[12], Meng Su[17], Hao-Ran Sun[3,4], Zhi-Yu Sun[12], Antonio Surdo[2], Xue-Jian Teng[13], Andrii Tykhonov[5], Gui-Fu Wang[3,4], Jin-Zhou Wang[9], Lian-Guo Wang[13], Shen Wang[10], Xiao-Lian Wang[3,4], Yan-Fang Wang[3,4], Da-Ming Wei[10,11], Jia-Ju Wei[10], Yi-Feng Wei[3,4], Di Wu[9], Jian Wu[10,11], Sha-Sha Wu[13], Xin Wu[5], Zi-Qing Xia[10], Zheng Xiong[6,7], En-Heng Xu[3,4], Hai-Tao Xu[13], Jing Xu[10], Zhi-Hui Xu[12], Zi-Zong Xu[3,4], Zun-Lei Xu[10], Guo-Feng Xue[13], Ming-Yu Yan[3,4], Hai-Bo Yang[12], Peng Yang[12], Ya-Qing Yang[12], Hui-Jun Yao[12], Yu-Hong Yu[12], Qiang Yuan[10,11], Chuan Yue[10], Jing-Jing Zang[10††], Sheng-Xia Zhang[12], Wen-Zhang Zhang[13], Yan Zhang[10], Ya-Peng Zhang[12], Yi Zhang[10,11], Yong-Jie Zhang[12], Yong-Qiang Zhang[10], Yun-Long Zhang[3,4], Zhe Zhang[10], Zhi-Yong Zhang[3,4], Cong Zhao[3,4], Hong-Yun Zhao[12], Xun-Feng Zhao[13], Chang-Yi Zhou[13], Xun Zhu[10‡‡], and Yan Zhu[13]

[1]Dipartimento di Matematica e Fisica E. De Giorgi, Università del Salento, I-73100, Lecce, Italy
[2]Istituto Nazionale di Fisica Nucleare (INFN) - Sezione di Lecce, I-73100, Lecce, Italy
[3]State Key Laboratory of Particle Detection and Electronics, University of Science and Technology of China, Hefei 230026, China
[4]Department of Modern Physics, University of Science and Technology of China, Hefei 230026, China
[5]Department of Nuclear and Particle Physics, University of Geneva, CH-1211, Switzerland
[6]Gran Sasso Science Institute (GSSI), Via Iacobucci 2, I-67100 L'Aquila, Italy
[7]Istituto Nazionale di Fisica Nucleare (INFN) - Laboratori Nazionali del Gran Sasso, I-67100 Assergi, L'Aquila, Italy
[8]University of Chinese Academy of Sciences, Beijing 100049, China
[9]Particle Astrophysics Division, Institute of High Energy Physics, Chinese Academy of Sciences, Beijing 100049, China
[10]Key Laboratory of Dark Matter and Space Astronomy, Purple Mountain Observatory, Chinese Academy of Sciences, Nanjing 210023, China
[11]School of Astronomy and Space Science, University of Science and Technology of China, Hefei 230026, China
[12]Institute of Modern Physics, Chinese Academy of Sciences, Lanzhou 730000, China
[13]National Space Science Center, Chinese Academy of Sciences, Nanertiao 1, Zhongguancun, Haidian district, Beijing 100190, China
[14]Istituto Nazionale di Fisica Nucleare, Sezione di Bari, via Orabona 4, I-70126 Bari, Italy
[15]Dipartimento di Fisica "M. Merlin", dell'Università e del Politecnico di Bari, via Amendola 173, I-70126 Bari, Italy
[16]Istituto Nazionale di Fisica Nucleare (INFN) - Sezione di Perugia, I-06123 Perugia, Italy
[17]Department of Physics and Laboratory for Space Research, the University of Hong Kong, Hong Kong SAR, China

*Now at Gran Sasso Science Institute (GSSI), Via Iacobucci 2, I-67100 L'Aquila, Italy.
†Now at Institute of Physics, Ecole Polytechnique Fédérale de Lausanne (EPFL), CH-1015 Lausanne, Switzerland.
‡Also at Dipartimento di Fisica e Geologia, Università degli Studi di Perugia, I-06123 Perugia, Italy.
§Now at Dipartimento di Fisica e Chimica "E. Segrè", Università degli Studi di Palermo, via delle Scienze ed. 17, I-90128 Palermo, Italy.
¶Now at Inter-university Institute for High Energies, Universitè Libre de Bruxelles, B-1050 Brussels, Belgium.
‖Now at Institute of Physics, Ecole Polytechnique Fédérale de Lausanne (EPFL), CH-1015 Lausanne, Switzerland.
**Now at New York University Abu Dhabi, Saadiyat Island, Abu Dhabi 129188, United Arab Emirates.
††Also at School of Physics and Electronic Engineering, Linyi University, Linyi 276000, China.
‡‡Also at School of computing, Nanjing University of Posts and Telecommunications, Nanjing 210023, China.

PoS(ICRC2025)061